Possibility of quantitative assessment of the contribution of paddy irrigation and caldera lakes to river water in Bali Island using water isotopic physics

Paddy and Water Environment
https://doi.org/10.1007/s10333-019-00742-1

ARTICLE

Possibility of quantitative assessment of the contribution of paddy irrigation and caldera lakes to river water in Bali Island using water isotopic physics

Takao Nakagiri[1] · Hisaaki Kato[2] · Seiji Maruyama[3] · Satoko Hashimoto[4] · Haruhiko Horino[1] · Shinji Sakurai[1]

Received: 29 October 2018 / Revised: 20 December 2018 / Accepted: 6 January 2019

Abstract
This study aims to investigate a possibility of quantitative assessment of the relationship between return flow from paddy fields and river regime by using hydrogen- and oxygen-isotopic ratios of water (i.e., δD and δ^{18}O). In the Saba River Basin and three caldera lakes (Tamblingan, Buyan, and Bratan) locating near the basin in the north of Bali Island, Indonesia, the δD and δ^{18}O in fresh rainwater, river water, spring water, the surface water of several paddy plots with ponding, and lake surface water were measured from 2012 to 2014. In the middle and the lower areas of this basin, paddy fields are predominant land use. In contrast, in the upper area, plantation and forest are major, while paddy fields are very limited. All the δD–δ^{18}O regression relationships in the upper river water, the spring water, and the fresh rainwater reasonably agreed with the Bali rainwater line (BRL), which is the "meteorological water line" specified for Bali (Kayane in water cycle and water use in Bali Island. Dissertation, Institute of Geoscience, University of Tsukuba, 1992). The regression lines for the paddy surface water [Paddy Line (PL)] and for the caldera lakes water (Lake Line), both of which had high correlation, could be significantly differentiated each other and also from the BRL. Almost all the plotted points of δ^{18}O vs. δD in the middle and the lower river waters containing discharge from paddy fields were located in a range between the BRL and the PL on a δ-diagram. Although further investigations are still needed, we concluded that it is possible to quantitatively assess the relationship between return flow from paddy fields and river regime, algebraically. In addition, according to the same logic, it was assumed with high possibility that the water in Lake Tamblingan adjacent to the Saba River Basin is flowing into the Panas River, which is a branch river of the Saba, beyond the basin boundary.

Keywords Paddy field · Return flow · River water · Water isotopic ratios · Quantitative assessment

Introduction

We heavily depend on river water as a water resource for agricultural, industrial, and domestic purposes. Continuous river water can also contribute to conserve aquatic ecosystems. River water stability, therefore, is very important from the view of water security and ecosystem conservation.

Paddy irrigation practices, especially in river basins where a large area of paddy fields are distributed, can significantly affect a river regime. While intake water volume from a river for paddy irrigation is usually large enough to predominate river flow, a considerable amount of irrigated water to paddy fields returns to the river after various time delays, such as several days or several months, and again becomes one of the components of river flow in the downstream. This means that the return flow from the paddy fields may contribute to stabilizing river flow even in

✉ Takao Nakagiri
nakagiri@envi.osakafu-u.ac.jp

[1] Graduate School of Life and Environmental Sciences, Osaka Prefecture University, 1-1 Gakuen-cho, Naka-ku, Sakai, Osaka 599-8531, Japan

[2] Division of Next Industry Generation, Department of Intellectual Property Research, Institute of Scientific and Industrial Research, Osaka University, ISIR Incubation Building Room I109, Mihogaoka 8-1, Ibaraki, Osaka 567-0047, Japan

[3] Kyoto Fission-Track Co., Ltd., 44-4 Oomiya Minami Tajiri-cho, Kita-ku, Kyoto 603-8832, Japan

[4] Center for Computational Sciences, University of Tsukuba, 1-1-1, Tennodai, Tsukuba, Ibaraki 305-8577, Japan

Published online: 04 April 2019

a nonirrigation season. Although this function has already been recognized and computer-model investigations and analyses have been conducted (e.g., OECD 2006), it is still very difficult to quantitatively assess the actual situation accurately because of the difficulty in identifying the return flow in river water.

As one possible idea to distinguish the return flow from the waters with different flow paths in river water, we focused on the following: (1) paddy water seems to have considerable exposure to evaporation on the surface compared with the other kinds of water; and (2) there is a definite change in the isotopic characteristic of water by the amount of evaporation exposed on the surface (Kendall and McDonnell 1998). In this study, we carried out hydrological surveys from 2012 to 2014 around the Saba River Basin located in the north of Bali Island, Indonesia. Using the obtained data, we investigated a possibility of quantitative assessment of the contribution of the return flow to river flow by using the hydrogen- and oxygen-isotopic ratios of water (i.e., δD and δ^{18}O). There are three caldera lakes near the basin (Lakes Tamblingan, Buyan, and Bratan). In this study, we also investigated the possibility of the contribution of these lakes to the river.

Materials and methods

Overview of the study area

Geography and land use

The study area is the Saba River Basin located in the northern seaside of Bali Island, Indonesia. Bali Island (8.06°S–8.85°S and 114.43°E–115.71°E) is in a tropical climate zone just to the south of the equator. The basin area is 131 km^2. Figure 1 shows the location and geographical shape of the basin. The Saba River flows into the northern sea from the mountainous area in the central part of the island and has many tributaries. Several representative tributaries are shown in Fig. 1a. There are three large caldera lakes (Bratan, Buyan, and Tamblingan) located to the east and just outside of the upper basin boundary. There are very few enclosed water areas such as irrigation ponds inside the basin.

The predominant land use in the basin is agricultural. In the lower area of the basin from midstream to downstream where the elevation is approximately < 500 m above sea level, most of the farmlands are paddy fields, and they are distributed over this area as shown in Fig. 1a. In the paddy fields in this basin, double or triple rice cropping through the year is commonly practiced. Although there is a dry season during which there is little rainfall for several months in Bali Island, in many paddy fields enough irrigation water is available mainly from the main or tributary rivers even during such periods.

In the highland area upstream, where the elevation is > 500 m above sea level, the farmland is mainly agroforestry, and tree crops such as coffee, cloves, and coconut are planted.

Intensive residential areas are limited in the downstream area.

Climatology and hydrology

The study area belongs to a tropical climate zone and has two seasons: wet (from approximately November to June) and dry (July to October). According to the measurement records at the center part of the basin from 2013 to 2015 (Saptomo et al. 2015), the monthly rainfall was 200–380 mm/month in the wet season and 0–100 mm/month in the dry season. The average daily evapotranspiration rate is 3 mm/day. The annual fluctuation of solar radiation is small because Bali Island is located close to the equator, and even during the wet season, there are many days with enough solar radiation to evaporate water in the daytime. Consequently, the daily evapotranspiration rate is relatively stable throughout the year.

Including the Saba River, most of the rivers in Bali Island are short and steep enough for the water to reach the mouth from upstream of the river within 1 day or at most 2 days.

Water sampling

In this study, on-site surveys for water sampling were carried out in six periods: (1) from September 1 to 2, 2012 (dry season); (2) from February 28 to March 1, 2013 (wet season); (3) from September 10 to 11, 2013 (dry season); (4) from December 13 to 17, 2013 (wet season); (5) from February 20 to 22, 2014 (wet season); and (6) from August 12 to 15, 2014 (dry season).

In the first three surveys during periods (1), (2), and (3), only the river water was sampled at four points on the Saba main stream and at four points on the four major tributaries (the Getas, the Bakah, the Titab, and the Panas), which are located just upstream from the confluence with the Saba main stream. In the last three surveys, additional water sampling points on the river streams (the Saba and the tributaries) were added. A total of 91 river water samples were obtained. The water samples were filtered with 0.2 μm-mesh membrane filters and preserved in glass vials (6 mL in volume).

In the surveys during periods (4), (5), and (6), paddy waters were also sampled at the upmost, around the middle, and the lower end in some paddy blocks, which consisted of several plots in different areas.

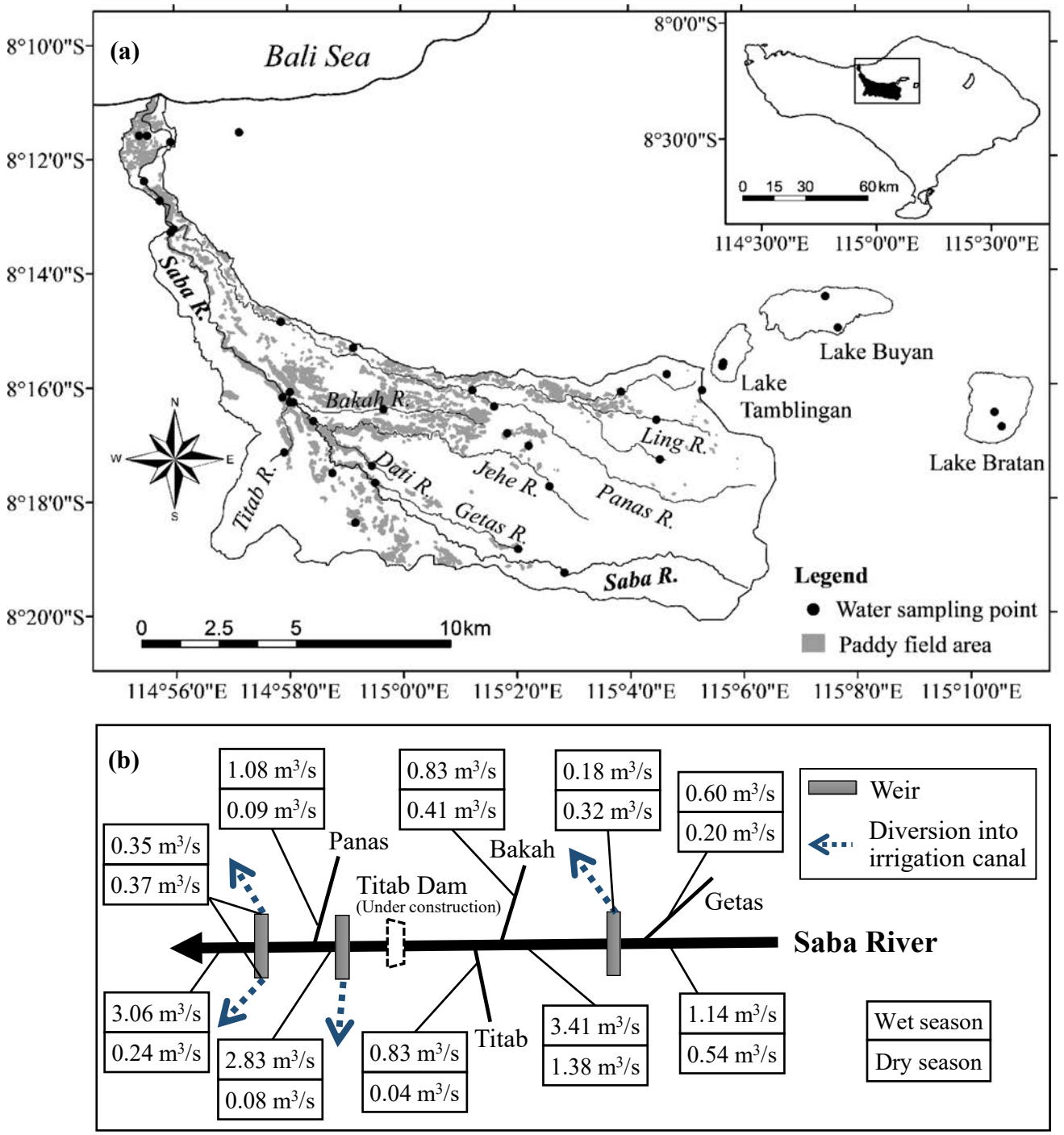

Fig. 1 Overview of the study area: **a** a map of the Saba River Basin and location of the water sampling points and **b** the mean river flows in the wet and the dry seasons at each point of the Saba River. The values of river flow were the mean of the observed data in February 2013 and in February 2014 for the wet season, and in August 2012 and in September 2013 for the dry season

Rainwaters were sampled in the surveys during periods (4) and (5), which were in the wet season. During these periods, plastic bottles were placed to collect rainwater at several points without any interception. The mouth of each plastic bottle was equipped with a plastic funnel through the use of a plastic ball to prevent the collected rainwater from evaporating. After rainfall, the bottles were collected within 1 day and the collected waters were poured into glass vials in the same method as the river water samples. A total of 13 rainwater samples were obtained.

In the surveys during periods (4) and (6), water sampling was carried out on three caldera lakes: Lakes Bratan, Buyan, and Tamblingan. The water was sampled at the center point of the water surface area in each lake at 5 m depths from the water surface to the lakebed or to 50 m in depth. A total of 23 lake water samples were obtained. The lake water samples were taken in the same manner as the river water samples.

The vials filled with the sample waters were cooled by coolant mediums in cooler boxes just after sampling. The vials were cooled in the refrigerator in the base camp close to the study site, and they were kept in the Styrofoam box in order to maintain low temperatures during transportation to Japan. The water samples were preserved in sample storage kept at 5 °C in the Research Institute for Humanity and Nature (RIHN), and analyses of the water isotopic ratios were carried out within 1 week of arrival.

Analyses of water stable isotopic ratios

Picarro L2120-i and L2130-i Cavity Ring-Down Spectrometers (CRDS) coupled with CTC LC-PAL liquid autosamplers were used for simultaneous analysis of the hydrogen and oxygen water isotopic ratios (i.e., δD and δ^{18}O) of the water samples at the RIHN. The δ value for D (deuterium) or ^{18}O is calculated by

$$\delta = \left(\frac{R_{\text{sample}}}{R_{\text{standard}}} - 1 \right) \times 1000 \ (‰) \tag{1}$$

where R_{sample} and R_{standard} are the ratios of the heavy isotope to the light one (e.g., ^{18}O/^{16}O) in the sampled water and the standard, respectively. The Standard Mean Ocean Water (SMOW) distributed by the International Atomic Energy Agency (IAEA) had previously been used for the standard material; however, it is no longer distributed. Presently, the Vienna-SMOW (VSMOW) is distributed by the IAEA as the standard material of analyses of the water isotopic ratios of unknown water samples.

In this study, the analyses were carried out according to the analytical procedures described by Maruyama and Tada (2014). Working standards distributed by Los Gatos Research, Inc. (hereafter abbreviated as LGR-WSs) were used for calibration of the analytical results. A set of three LGR-WSs (i.e., #3, #4, and #5), covering −79 to −9.8‰ of δD and −11.5 to −3.0‰ of δ^{18}O for calibration, were normally used for calibration of the measurement values of the water samples obtained from Bali Island. The standard errors (1σmean) of the analytical values of δD and δ^{18}O obtained in this study were typically less than ±0.2‰ and less than ±0.04‰, respectively. Additional details are described in Maruyama and Tada (2014).

Results and discussion

Table 1 lists the location of the sampling points of water and the obtained data of the water isotopic ratios. In this study, the water samples were categorized into four groups: (1) rainwater, waterfall, and spring water, (2) caldera lake water, (3) paddy water, and (4) river water. The mean values and the standard deviations (SDs) of the water isotopic ratios ($\delta D_{\text{mean} \pm \text{SD}}$ and $\delta^{18}O_{\text{mean} \pm \text{SD}}$) in each group were: (1) −44.9 ± 17.2 and −7.34 ± 2.32, (2) −26.0 ± 16.2 and −4.12 ± 1.02, (3) −28.9 ± 4.9 and −5.04 ± 0.83, and (4) −33.3 ± 4.4 and −5.95 ± 0.64, respectively. The water samples in group (1) had the smallest values both in the δD_{mean} and the $\delta^{18}O_{\text{mean}}$ and had the largest SDs of them. On the other hand, those in group (4) had the largest mean values and the smallest SDs. The features in water isotopic ratios are considered in each group below. Furthermore, relationship between the river water and return flow from paddy fields is also discussed.

Rainwater, waterfall, and spring water

Figure 2a shows plots of the water isotopic ratios in the samples of rainwater, waterfall, and spring water on a δ-diagram. In this figure, the rainwater line for Bali Island, which is a regression line obtained from more rainwater data in Bali Island by Kayane (1992) and represented as "BRL" (Bali Rainwater Line), is also shown. The BRL is defined as the following equation:

$$\delta D = 8\delta^{18}O + 17 \tag{2}$$

Craig (1961) reported that the relationship between δ^{18}O and δD in rainwaters sampled over the world can be expressed by the following equation:

$$\delta D = 8\delta^{18}O + 10 \tag{3}$$

This equation is called the "Global Meteoric Water Line" (GMWL, or just MWL) (Kendall and McDonnell 1998). Compared the two Eqs. (2) and (3), their slope values are the same, but their intercept values, which are called the "deuterium excess" (or *d* excess, or *d* parameter), are different. It is known that the *d*-excess value varies depending on the region or the regional meteorological condition, while the slope value of 8 is approximately constant (Kendall and McDonnell 1998).

The plots of the water isotopic ratios of the rainwater samples obtained in the surveys for this study had a tendency to be slightly lower than the BRL by up to ~ 1.5‰ in δ^{18}O. It leads to be derived a regression line with smaller slope value (7.1) than that of the BRL, as shown in Fig. 2a. To have a smaller slope value than that

Table 1 List of the location of the sampling points and the obtained data of the water isotopic ratios

Sample ID	Date	Lat. (S)	Lng. (E)	$\delta^{18}O$	δD
Rain_1	16-Dec-13	8°17′01.2″	115°02′12.2″	−11.74	−76.3
Rain_2	17-Dec-13	8°16′16.3″	114°58′02.8″	−11.32	−75.2
Rain_3	17-Dec-13	8°12′42.4″	114°55′45.3″	−9.47	−61.7
Rain_4	17-Dec-13	8°11′36.3″	114°55′22.1″	−10.71	−71.0
Rain_5	5-Feb-14	8°15′51.8″	115°05′27.0″	−8.82	−57.5
Rain_6	5-Feb-14	8°17′01.9″	115°02′14.9″	−7.48	−44.9
Rain_7	5-Feb-14	8°16′08.5″	114°57′57.9″	−5.71	−34.0
Rain_8	22-Feb-14	8°17′32.2″	114°58′40.2″	−5.24	−30.6
Rain_9	22-Feb-14	8°16′08.8″	114°57′57.8″	−6.35	−41.4
Rain_10	24-Feb-14	8°11′36.3″	114°55′22.1″	−3.34	−21.5
Rain_11	25-Feb-14	8°13′14.8″	114°55′55.6″	−7.82	−49.7
Rain_12	27-Feb-14	8°17′01.9″	115°02′14.9″	−5.62	−30.6
Rain_13	3-Mar-14	8°17′01.9″	115°02′14.9″	−5.69	−29.5
WF_1	16-Dec-13	8°15′47.8″	115°04′40.2″	−8.62	−52.7
WF_2	17-Dec-13	8°19′16.1″	115°02′50.0″	−6.56	−35.9
SPRG_1	17-Dec-13	8°19′16.1″	115°02′50.0″	−5.98	−31.8
SPRG_2	20-Feb-14	8°19′16.0″	115°02′49.5″	−5.80	−31.8
SPRG_3	15-Aug-14	8°19′16.0″	115°02′49.4″	−5.93	−32.5
Lake-Br_1	14-Dec-13	8°16′45.1″	115°10′31.6″	−3.12	−20.2
Lake-Br_2	14-Dec-13	8°16′47.3″	115°10′28.1″	−2.83	−18.6
Lake-Br_3	15-Aug-14	8°16′29.0″	115°10′26.2″	−2.68	−18.0
Lake-Br_4	15-Aug-14	8°16′29.0″	115°10′26.2″	−2.69	−18.0
Lake-Br_5	15-Aug-14	8°16′29.0″	115°10′26.2″	−2.69	−18.0
Lake-Br_6	15-Aug-14	8°16′29.0″	115°10′26.2″	−2.72	−18.0
Lake-Br_7	15-Aug-14	8°16′29.0″	115°10′26.2″	−2.71	−18.1
Lake-Br_8	15-Aug-14	8°16′29.0″	115°10′26.2″	−2.68	−18.1
Lake-By_1	14-Dec-13	8°14′59.9″	115°07′40.6″	−5.14	−31.3
Lake-By_2	14-Dec-13	8°14′59.9″	115°07′40.6″	−4.99	−30.2
Lake-By_3	15-Aug-14	8°14′26.7″	115°07′27.7″	−4.86	−30.0
Lake-By_4	15-Aug-14	8°14′26.7″	115°07′27.7″	−4.88	−30.1
Lake-By_5	15-Aug-14	8°14′26.7″	115°07′27.7″	−4.91	−30.2
Lake-By_6	15-Aug-14	8°14′26.7″	115°07′27.7″	−4.88	−30.1
Lake-By_7	15-Aug-14	8°14′26.7″	115°07′27.7″	−4.88	−30.2
Lake-By_8	15-Aug-14	8°14′26.7″	115°07′27.7″	−4.93	−30.3
Lake-By_9	15-Aug-14	8°14′26.7″	115°07′27.7″	−5.03	−30.8
Lake-Tm_1	14-Dec-13	8°15′38.1″	115°05′37.3″	−5.05	−31.7
Lake-Tm_2	14-Dec-13	8°15′38.1″	115°05′37.3″	−4.67	−29.7
Lake-Tm_3	15-Aug-14	8°15′36.6″	115°05′39.5″	−4.57	−29.3
Lake-Tm_4	15-Aug-14	8°15′36.6″	115°05′39.5″	−4.60	−29.3
Lake-Tm_5	15-Aug-14	8°15′36.6″	115°05′39.5″	−4.56	−29.2
Lake-Tm_6	15-Aug-14	8°15′36.6″	115°05′39.5″	−4.57	−29.2
Paddy_1	13-Dec-13	8°16′21.4″	114°58′01.0″	−5.70	−32.0
Paddy_2	13-Dec-13	8°16′16.3″	114°58′02.9″	−5.52	−31.2
Paddy_3	13-Dec-13	8°16′13.5″	114°58′03.5″	−5.57	−31.5
Paddy_4	22-Feb-14	8°17′02.3″	115°02′14.0″	−6.63	−38.0
Paddy_5	22-Feb-14	8°17′00.8″	115.2°02′11.0″	−5.57	−33.6
Paddy_6	22-Feb-14	8°17′01.3″	115°02′10.9″	−4.20	−27.0
Paddy_7	22-Feb-14	8°18′23.4″	114°59′10.6″	−5.77	−32.5
Paddy_8	22-Feb-14	8°18′22.6″	114°59′09.5″	−5.63	−31.8
Paddy_9	22-Feb-14	8°18′22.2″	114°59′08.8″	−5.53	−31.0
Paddy_10	22-Feb-14	8°16′11.5″	114°57′54.5″	−5.13	−28.9

Table 1 (continued)

Sample ID	Date	Lat. (S)	Lng. (E)	$\delta^{18}O$	δD
Paddy_11	22-Feb-14	8°16′11.0″	114°57′55.3″	−4.51	−26.6
Paddy_12	22-Feb-14	8°16′09.6″	114°57′55.3″	−4.55	−26.8
Paddy_13	13-Aug-14	8°16′11.2″	114°57′53.9″	−4.23	−23.0
Paddy_14	13-Aug-14	8°16′09.9″	114°57′52.7″	−4.02	−21.9
Paddy_15	13-Aug-14	8°16′10.1″	114°57′53.3″	−3.70	−19.8
Paddy_16	14-Aug-14	8°15′17.6″	114°59′07.1″	−5.91	−34.4
Paddy_17	14-Aug-14	8°15′19.2″	114°59′08.0″	−5.74	−33.3
Paddy_18	14-Aug-14	8°15′20.4″	114°59′07.5″	−5.49	−31.7
Paddy_19	14-Aug-14	8°11′35.4″	114°55′30.3″	−4.46	−25.6
Paddy_20	14-Aug-14	8°11′34.9″	114°55′31.3″	−4.01	−23.1
Paddy_21	14-Aug-14	8°11′34.3″	114°55′30.4″	−3.95	−22.9
Riv-S-1	17-Dec-13	8°19′16.4″	115°03′00.5″	−6.56	−36.0
Riv-S-2_1	20-Feb-14	8°19′15.7″	115°02′49.6″	−6.08	−33.9
Riv-S-2_2	15-Aug-14	8°19′15.7″	115°02′49.6″	−5.79	−31.8
Riv-S-3_1	1-Sep-12	8°17′41.9″	114°59′30.8″	−6.07	−32.8
Riv-S-3_2	28-Feb-13	8°17′41.9″	114°59′30.8″	−6.11	−32.9
Riv-S-3_3	11-Sep-13	8°17′41.9″	114°59′30.8″	−5.96	−31.6
Riv-S-3_4	15-Dec-13	8°17′41.9″	114°59′30.8″	−6.07	−32.7
Riv-S-3_5	20-Feb-14	8°17′41.9″	114°59′30.8″	−5.83	−32.1
Riv-S-3_6	15-Aug-14	8°17′41.9″	114°59′30.8″	−5.66	−30.5
Riv-S-4_1	15-Dec-13	8°17′40.4″	114°59′29.6″	−6.20	−33.6
Riv-S-4_2	20-Feb-14	8°17′40.4″	114°59′29.6″	−5.86	−32.2
Riv-S-4_3	15-Aug-14	8°17′40.4″	114°59′29.6″	−5.66	−30.5
Riv-S-5_1	15-Dec-13	8°16′35.1″	114°58′25.3″	−5.95	−32.2
Riv-S-5_2	20-Feb-14	8°16′35.1″	114°58′25.3″	−5.61	−31.2
Riv-S-5_3	15-Aug-14	8°16′35.1″	114°58′25.3″	−5.40	−29.6
Riv-S-6_1	15-Dec-13	8°16′34.6″	114°58′24.9″	−5.95	−32.3
Riv-S-6_2	20-Feb-14	8°16′34.6″	114°58′24.9″	−5.67	−31.6
Riv-S-6_3	15-Aug-14	8°16′34.6″	114°58′24.9″	−5.34	−29.7
Riv-S-7_1	1-Sep-12	8°16′19.0″	114°58′08.6″	−5.57	−30.5
Riv-S-7_2	28-Feb-13	8°16′19.0″	114°58′08.6″	−5.95	−32.3
Riv-S-7_3	11-Sep-13	8°16′19.0″	114°58′08.6″	−5.67	−30.6
Riv-S-7_4	14-Dec-13	8°16′19.0″	114°58′08.6″	−7.86	−47.8
Riv-S-7_5	20-Feb-14	8°16′19.0″	114°58′08.6″	−5.66	−31.5
Riv-S-7_6	15-Aug-14	8°16′19.0″	114°58′08.6″	−5.44	−29.8
Riv-S-8_1	14-Dec-13	8°16′17.6″	114°58′07.8″	−7.20	−42.5
Riv-S-8_2	20-Feb-14	8°16′17.6″	114°58′07.8″	−5.65	−31.9
Riv-S-8_3	15-Aug-14	8°16′17.6″	114°58′07.8″	−5.50	−30.5
Riv-S-9	15-Dec-13	8°16′09.3″	114°57′59.1″	−6.01	−33.3
Riv-S-10_1	15-Dec-13	8°16′08.2″	114°57′56.9″	−5.99	−32.8
Riv-S-10_2	20-Feb-14	8°16′08.2″	114°57′56.9″	−5.72	−31.9
Riv-S-10_3	15-Aug-14	8°16′08.2″	114°57′56.9″	−5.47	−30.2
Riv-S-11_1	2-Sep-12	8°13′15.1″	114°55′57.2″	−5.52	−30.4
Riv-S-11_2	1-Mar-13	8°13′15.1″	114°55′57.2″	−5.86	−32.0
Riv-S-11_3	10-Sep-13	8°13′15.1″	114°55′57.2″	−5.55	−30.5
Riv-S-11_4	16-Dec-13	8°13′15.1″	114°55′57.2″	−6.26	−34.7
Riv-S-11_5	21-Feb-14	8°13′15.1″	114°55′57.2″	−5.49	−31.1
Riv-S-11_6	15-Aug-14	8°13′15.1″	114°55′57.2″	−5.35	−29.8
Riv-S-12_1	16-Dec-13	8°13′11.7″	114°55′58.5″	−6.67	−38.6
Riv-S-12_2	21-Feb-14	8°13′11.7″	114°55′58.5″	−5.79	−33.0
Riv-S-12_3	15-Aug-14	8°13′11.7″	114°55′58.5″	−5.38	−30.2

Table 1 (continued)

Sample ID	Date	Lat. (S)	Lng. (E)	$\delta^{18}O$	δD
Riv-S-13_1	31-Aug-12	8°12′22.4″	114°55′28.4″	−5.47	−30.8
Riv-S-13_2	28-Feb-13	8°12′22.4″	114°55′28.4″	−6.04	−33.5
Riv-S-13_3	10-Sep-13	8°12′22.4″	114°55′28.4″	−5.54	−30.9
Riv-S-13_4	21-Feb-14	8°12′22.4″	114°55′28.4″	−5.56	−32.0
Riv-S-13_5	15-Aug-14	8°12′22.4″	114°55′28.4″	−5.29	−30.1
Riv-S-14	15-Dec-13	8°11′45.0″	114°55′53.7″	−6.65	−39.0
Riv-S-15_1	21-Feb-14	8°11′33.8″	114°55′56.9″	−5.57	−31.8
Riv-S-15_2	15-Aug-14	8°11′33.8″	114°55′56.9″	−5.19	−29.6
Riv-TG-1	17-Dec-13	8°17′42.9″	114°59′35.2″	−6.27	−34.2
Riv-TG-2_1	1-Sep-12	8°17′41.1″	114°59′30.8″	−5.95	−31.4
Riv-TG-2_2	28-Feb-13	8°17′41.1″	114°59′30.8″	−6.12	−33.1
Riv-TG-2_3	11-Sep-13	8°17′41.1″	114°59′30.8″	−6.05	−32.4
Riv-TG-2_4	15-Dec-13	8°17′41.1″	114°59′30.8″	−6.23	−33.8
Riv-TG-2_5	20-Feb-14	8°17′41.1″	114°59′30.8″	−5.90	−32.8
Riv-TG-2_6	15-Aug-14	8°17′41.1″	114°59′30.8″	−5.76	−31.5
Riv-TD-1	16-Dec-13	8°17′22.1″	115°02′05.9″	−6.89	−38.2
Riv-TD-2	17-Dec-13	8°17′05.5″	114°59′11.2″	−6.34	−35.1
Riv-TD-3_1	15-Dec-13	8°16′34.8″	114°58′25.7″	−6.02	−33.4
Riv-TD-3_2	20-Feb-14	8°16′34.8″	114°58′25.7″	−5.65	−32.0
Riv-TD-3_3	15-Aug-14	8°16′34.8″	114°58′25.7″	−5.36	−29.7
Riv-TB-1	16-Dec-13	8°16′48.6″	115°01′52.6″	−6.40	−36.7
Riv-TB-2	17-Dec-13	8°16′23.1″	114°59′39.4″	−6.51	−36.7
Riv-TB-3_1	1-Sep-12	8°16′18.0″	114°58′08.6″	−6.06	−33.9
Riv-TB-3_2	28-Feb-13	8°16′18.0″	114°58′08.6″	−6.24	−34.7
Riv-TB-3_3	11-Sep-13	8°16′18.0″	114°58′08.6″	−6.10	−34.0
Riv-TB-3_4	14-Dec-13	8°16′18.0″	114°58′08.6″	−7.86	−47.7
Riv-TB-3_5	20-Feb-14	8°16′18.0″	114°58′08.6″	−5.87	−33.7
Riv-TB-3_6	15-Aug-14	8°16′18.0″	114°58′08.6″	−5.78	−33.0
Riv-TT-1	17-Dec-13	8°16′38.4″	114°57′55.4″	−5.83	−31.6
Riv-TT-2_1	1-Sep-12	8°16′09.8″	114°57′59.2″	−4.72	−25.8
Riv-TT-2_2	28-Feb-13	8°16′09.8″	114°57′59.2″	−5.60	−30.2
Riv-TT-2_3	11-Sep-13	8°16′09.8″	114°57′59.2″	−4.77	−25.7
Riv-TT-2_4	15-Dec-13	8°16′09.8″	114°57′59.2″	−5.83	−31.5
Riv-TT-2_5	20-Feb-14	8°16′09.8″	114°57′59.2″	−5.28	−29.9
Riv-TT-2_6	13-Aug-14	8°16′09.8″	114°57′59.2″	−4.30	−23.6
Riv-TP-1	16-Dec-13	8°16′05.3″	115°03′52.2″	−7.03	−40.3
Riv-TP-2	16-Dec-13	8°16′11.9″	115°02′59.7″	−8.86	−55.2
Riv-TP-3	16-Dec-13	8°16′07.3″	115°01′15.8″	−6.70	−37.8
Riv-TP-4_1	21-Feb-14	8°16′03.8″	115°01′14.1″	−6.30	−36.0
Riv-TP-4_2	15-Aug-14	8°16′03.8″	115°01′14.1″	−6.21	−35.7
Riv-TP-5	16-Dec-13	8°14′51.9″	114°57′51.6″	−6.62	−38.1
Riv-TP-6_1	21-Feb-14	8°14′53.5″	114°57′51.5″	−5.95	−34.6
Riv-TP-6_2	15-Aug-14	8°14′53.5″	114°57′51.5″	−5.69	−32.7
Riv-TP-7_1	16-Dec-13	8°13′13.3″	114°55′58.9″	−6.86	−40.0
Riv-TP-7_2	20-Feb-14	8°13′13.3″	114°55′58.9″	−5.78	−33.8
Riv-TP-7_3	15-Aug-14	8°13′13.3″	114°55′58.9″	−5.38	−31.1
Riv-TP-7_4	2-Sep-12	8°13′13.3″	114°55′58.9″	−5.72	−31.7
Riv-TP-7_5	1-Mar-13	8°13′13.3″	114°55′58.9″	−6.08	−34.1
Riv-TP-7_6	10-Sep-13	8°13′13.3″	114°55′58.9″	−5.61	−31.9
Riv-TL-1_1	21-Feb-14	8°16′00.7″	115°01′16.0″	−6.26	−36.6
Riv-TL-1_2	15-Aug-14	8°16′00.7″	115°01′16.0″	−6.29	−36.7

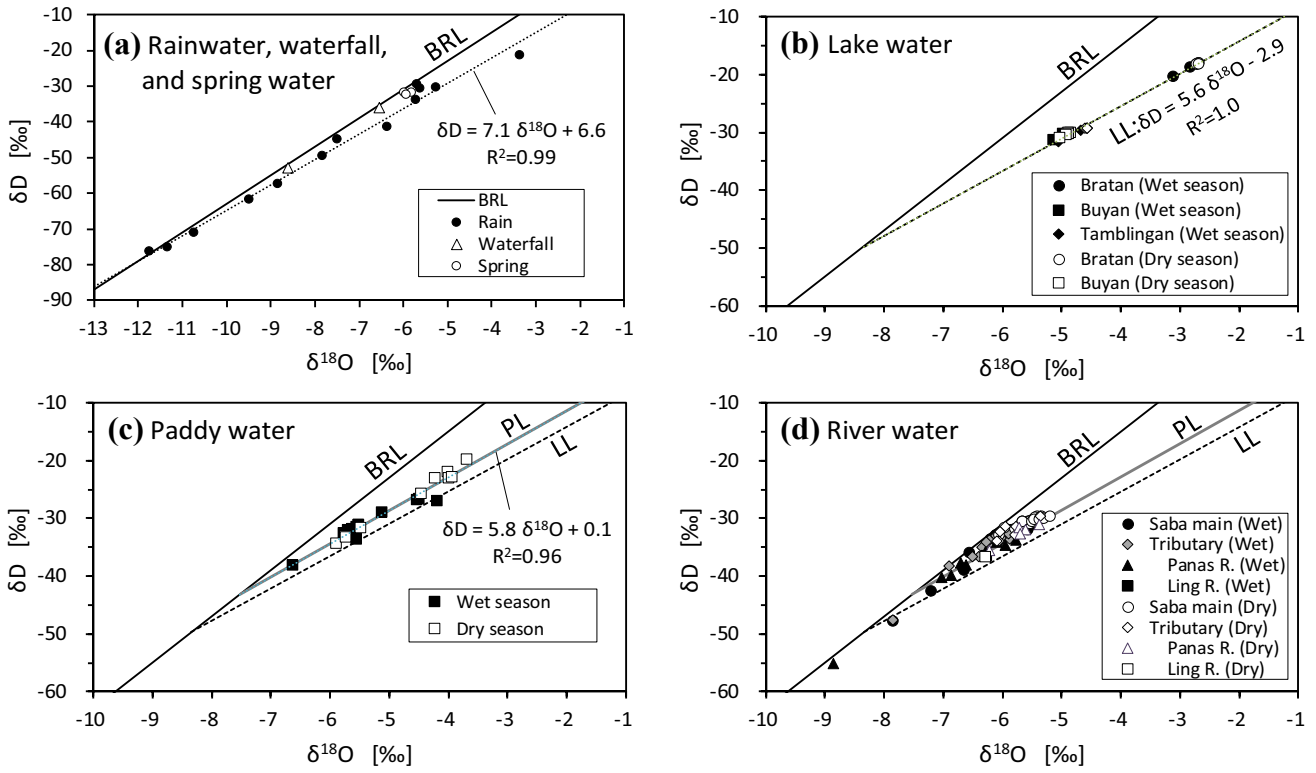

Fig. 2 δ-diagrams of **a** rain, waterfall, and spring waters and the Bali rainwater line (BRL, $\delta D = 8\ d^{18}O + 17$) by Kayane (1992), **b** the caldera lakes, **c** the paddy waters, and **d** the waters obtained from the Saba River and its tributaries. The sizes of errors ($1\sigma_{mean}$) of the water isotopic ratios (δD and $\delta^{18}O$) of each sample were almost equivalent to or smaller than that of the symbol. Filled and open symbols represent the samples obtained in the wet and the dry seasons, respectively. The abbreviations are defined as follows: BRL is the Bali rain line, LL is the lake line, and PL is the paddy line. Though there were three plots in the region below the LL, two of the three overlapped around ($\delta^{18}O$, δD) = (−7.9, −48)

of the MWL means that the rainwater might be exposed to evaporation after reaching the land surface. In the surveys for this study, plastic bottles to collect rainwater were set at several sites without shade and left, in some cases, under sunshine for several hours before the collected rainwater was sampled into a glass vial. In other words, some rainwater samples might have been influenced by evaporation.

On the other hand, the plots of the samples from the waterfall and the spring are almost on the BRL. The waterfall appeared only after consecutive rainfall events or a heavy rainfall event in the wet season. The spring is located in a deep forest area upstream of the basin, and the water flow volume was almost constant throughout the year. It is assumed that the waters of the waterfall and the spring were not exposed to evaporation on the land surface for a prolonged period. In this study, therefore, we assumed that the BRL should be appropriate as the MWL of Bali Island for the following discussions.

Caldera lake water

In this study, the water samples were obtained from three of five caldera lakes in Bali Island: Lakes Bratan, Buyan, and Tamblingan. These caldera lakes have a closed system, and Shimano (1994) argued that there is no surface outflow from these lakes. The water areas of Lakes Bratan, Buyan, and Tamblingan are 383 ha, 471 ha, and 150 ha, respectively. The locational relationship of these lakes is shown in Fig. 1a.

The water isotopic ratios of the water samples obtained from the three caldera lakes are shown in Fig. 2b. The water isotopic ratios from each lake were similar to each other, and the $\delta^{18}O$ values ranged within 0.5‰. Moreover, the water isotopic ratios of each caldera lake obtained in the dry season were similar to those obtained in the wet season (Fig. 2b). All values of the water isotopic ratios of the caldera lakes were plotted along a single regression line, defined as the "Lake Line (LL)" here. The coefficient of determination (R^2) of the LL was almost 1.0, and the properties of the water

isotopic ratios of the caldera lakes could be interpreted by using the LL.

The water isotopic ratios of Lake Buyan were similar to those of Lake Tamblingan, whereas those of Lake Bratan were ~ 2.0‰ heavier in $\delta^{18}O$ than Lakes Buyan and Tamblingan (Fig. 2b). Lakes Buyan and Tamblingan are isolated by cliffs that are > 100 m high on the northern side. The cliffs can shade the water surface of these two lakes from the sun, and the moist air from the surfaces of the lakes is also difficult to exchange with relatively dry air on the surrounding land areas. On the other hand, moist air from the surface of Lake Bratan can be relatively easily exchanged with the surrounding dry air, and there is no shade on the surface of Lake Bratan in the daytime due to the absence of high cliffs surrounding the lake. Therefore, Lake Bratan can evaporate and experience the isotopic fractionation effect more strongly than Lakes Buyan and Tamblingan, resulting in water isotopic ratios that were heavier than the other two caldera lakes.

The lake waters were sampled from the surface to a depth of 25 m in Lake Bratan, from the surface to a depth of 50 m in Lake Buyan, and from the surface to a depth of 20 m in Lake Tamblingan. The water isotopic ratios of the water samples from various depths from each caldera lake had no statistical significant difference. Moreover, as shown in Fig. 2b, the water isotopic ratios of each lake obtained in the wet season had also almost no statistically significant difference from those obtained in the dry season. These results suggested that the water isotopic ratios of these three caldera lakes were maintained at a constant level throughout the year by advection and diffusion transport mechanisms in the lakes.

These caldera lakes may have experienced a dynamic evaporation (nonequilibrium fractionation) effect for a long duration among the surface waters, which could have been incorporated into the river waters. Therefore, the water isotopic ratios of each caldera lake were thought to be in an almost steady state, and the LL shown in Fig. 2b could be regarded as the convergence of the water isotopic ratios archived by the evaporation effect on Bali Island.

Paddy water

The water isotopic ratios of the paddy waters obtained from the paddy fields in or near the Saba River Basin are plotted in Fig. 2c. The plots were observed to scatter more widely than those of the caldera lakes. Paddy rice cultivation requires a large amount of irrigation water throughout the cropping period, and a wide variety of waters, such as rainwater, groundwater, and return flow from paddy fields in the upper stream areas, could potentially be incorporated into the paddy water. Moreover, paddy water can be affected by the evaporation effect in varying degrees and can flow out to be incorporated into the river water or the groundwater again. Therefore, the paddy water and the water affected by paddy water may have highly variable water isotopic ratios. Considering this variability of paddy waters, the scattering of the water isotopic ratios of paddy waters seemed to be rather reasonable.

While the water isotopic ratios of the paddy waters were scattered to some extent, they still generally plotted along a single regression line, defined as the "Paddy Line (PL)" ($R^2 = 0.96$). Moreover, the water isotopic ratios of the paddy waters obtained in both the dry and wet seasons were generally very close to the PL. This suggests that there may have been no remarkable difference in the isotopic fractionation process of the paddy waters between the dry and wet seasons. We concluded that the properties of the water isotopic ratios of the paddy waters in the Saba River Basin could also be interpreted by using the PL, as well as the isotopic properties of the caldera lakes.

As shown in Fig. 2c, almost all of the plots were in the region between the BRL and the LL. The more the rainwater is affected by the dynamic evaporation effect, the heavier it becomes, and the plot determined by its isotopic ratios will diverge from the BRL and approach the LL; thus, the LL is regarded as a convergence archived by the evaporation effect in Bali Island. This result indicates that the water isotopic ratios of rainwaters affected by any amount of evaporation in natural conditions should be theoretically plotted in this region. Assuming that the paddy water was a general mixture of several waters, all of which originated from rainwater and had varying degrees of evaporation experience and also received the dynamic isotopic fractionation effect by evaporation on the paddy plots; then, almost all of the water isotopic ratios of the paddy waters would be expected to be plotted in this region.

River water

The water isotopic ratios of the samples obtained from the Saba River and its tributaries are plotted and distinguished by season in Fig. 2d. Note that for the discussion mentioned below, different styles of symbols were employed for the Panas River and the Ling River (one of the tributaries of the Panas River), though they are both tributaries of the Saba River (Fig. 1a).

In Fig. 2d, almost all of the plots are within the region between the BRL and the LL, and besides, the majority of them are in the region between the BRL and the PL. Algebraically, if two kinds of waters with different water isotopic ratios, both of which are plotted in a region between two straight lines that are not parallel to each other, are mixed together, then the isotopic ratios of the mixed water would also be plotted within the same region. Considering the site situation that there was no significant surface water except

for paddy water and surface discharge (such as a temporal waterfall) just after rainfall inside the basin, most river waters in this basin were assumed to basically consist of two kinds of waters with the properties of the BRL or the PL.

On the other hand, in Fig. 2d, there are some plots in the region on or below the PL and above the LL. The water isotopic ratios above the PL could be explained by a linear combination of the meteoric waters and the paddy waters, whereas those on or below the PL could not be explained reasonably. If the water isotopic ratios of the river water were plotted just on the PL, then this means that all of the river water must have originated in the paddy water, though this is impossible in the actual situation of the Saba River. Moreover, if the ratios were below the PL, then no possible mathematical explanation exists. Almost all of the plots on or below the PL were from water samples obtained from the Panas River and the Ling River. The caldera lakes are located at the uppermost stream of the Ling River, though they are outside of the Saba River Basin boundary. Since these plots were still above the LL, they could be explained by incorporating the LL. For this reason, the water in the caldera lakes was assumed to have flowed into the Ling River and consequently into the Panas River beyond the basin boundary through the underground. Also, the quantity of the inflow was thought to be very stable because the river flows in the Ling and Panas Rivers in the dry season were very stable. Considering the terrain conditions, there appeared to be no inflow from the caldera lakes into the Saba River and the other tributaries, except for the Panas and Ling Rivers.

As shown in Fig. 1a, after joining between the Panas River and the main stream of the Saba River, the quantity of the Panas River flow accounted for 1/2 (in the dry season) to 1/3 (in the wet season) of the Saba River flow. The contribution of the Panas River to the Saba River flow was considerable, especially in the dry season. Consequently, the caldera lakes could possibly be contributing to the stabilization of the Saba River flow, especially in the lower reaches in the dry season.

Three of the plots were out of the region between the BRL and the LL, but very close to the BRL on the left side of the graph area in Fig. 2d. Note that two of the three plots were plotted around $(\delta^{18}O, \delta D) = (-7.9, -48)$ and thus were overlapped, so there appears to be only two plots in this region. Among these plots, one was obtained from the upper stream of the Panas, another was from the Bakah at the joining point between this tributary and the main stream of the Saba around the middle area of the basin, and the third was from the main stream of the Saba at the point very close to the second one. All of the water samples in these regions were taken while under the influence of large, direct runoff by consecutive heavy rainfalls from December 13 to 16, 2013 (93 mm in total; 43 mm/h at the peak). Therefore, rainwater accounted for a very large portion of these river water samples.

Relationship between the river water and return flow from paddy fields

As mentioned above, there appeared to be no area into which the caldera lake water flowed in the Saba River Basin, with the exception of the Panas River (including the Ling River) basin, and the river water in the basin was assumed to be basically composed of the meteoric waters and return flow waters from the paddy fields. The meteoric waters contain not only "fresh" rainwater, but also all of the different types of waters that had properties explained by the BRL such as the direct runoff (water that flows over the ground surface or through the ground directly into the river streams after rainfall) and the spring water.

Figure 3 shows the relationship between the ratios of the paddy field area to each sub-basin area (basin area of the tributaries), and the relative positions of the water isotopic ratios to the BRL and the PL by season. We excluded the water isotopic ratios of the water samples taken from the Panas River and its tributary (i.e., the Ling River), which were assumed to be strongly influenced by the lake waters,

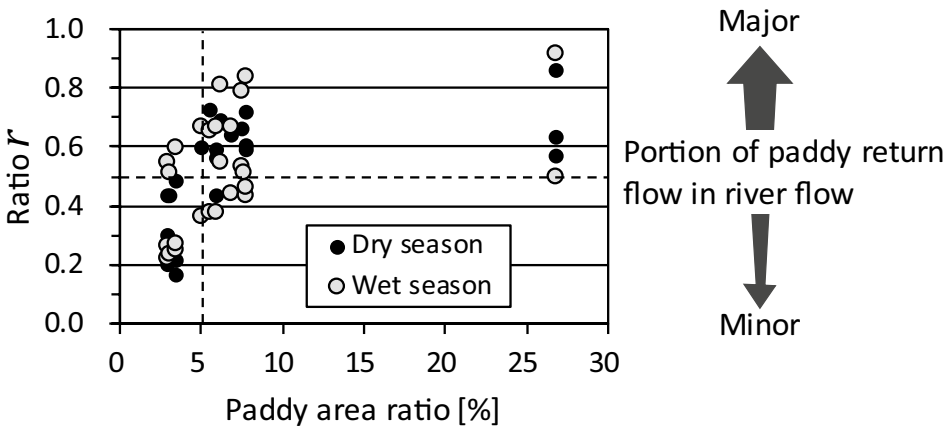

Fig. 3 The relationship between the area ratios of paddies in each sub-basin and the positions of the water isotopic ratios relative to the BRL and the PL shown in Fig. 2

and the water samples in which rainwater was considerably dominated by heavy rainfalls. The ratio r in Fig. 3 is defined as follows:

$$r = l_1/(l_1 + l_2) \quad (4)$$

where l_1 is the distance from each plot to the BRL and l_2 is the distance from each plot to the PL in Fig. 2d. The larger the value of r for a certain plot becomes, the relatively closer the plot approaches the PL; namely, the constituent ratio of paddy water to the river water becomes theoretically higher.

In Fig. 3, for the smaller ratios of paddy area (approximately less than 5%), most of the r values were less than 0.5, whereas for the larger ratios (approximately greater than 5%), even though it was 27% at most, the r values were mostly over 0.5 all thorough the year. Therefore, the paddy water was assumed to account for more than half of the river flow when the r value was over 0.5. This indicates that the paddy fields above a certain area size could significantly contribute to the river flow by the return flow from them to extend beyond their area ratios.

The distribution of the r values of the dry season is slightly smaller than that of the wet season for each paddy area ratio, although they almost completely overlap each other (Fig. 3). This difference may be due to rainfall during the wet season. When there is considerable surface runoff due to relatively heavy rainfall, the r value becomes smaller. On the other hand, rainfall on the paddy field can increase the return flow and that can lead to the higher r value when there is less surface flow during the wet season.

Conclusion

In this study, the linear algebraic characteristics of the water isotopic ratios of rainwater, river water, and paddy water in the Saba River Basin and three caldera lakes adjacent to this basin were investigated. The water isotopic ratios of the samples obtained from Bali Island exhibited the characteristics according to the fundamental principle that all surface waters originated in the meteoric waters, and that they are isotopically fractionated by evaporation effects (e.g., Alley and Cuffey 2001). The water isotopic ratios of rainwaters, the caldera lake waters, and paddy waters could also be explained by specific linear isotope lines.

The relationship among these characteristics was investigated to reveal that the water isotopic ratios of river water could be expressed by a linear combination of the ratios. Furthermore, the results suggested that there was likely to be a stable inflow from the caldera lakes, which are located outside the basin area, to the Saba River through its tributaries (i.e., the Panas and Ling Rivers). In particular, in the lower reach from the joining point between the Panas River and the main stream of the Saba, the contribution of the caldera lake waters to the river flow appeared to be significant. Previous reports by Kayane (1992) and Shimano (1994) provided no evidence for a relationship between the caldera lakes and the neighboring rivers in Bali Island, despite their considerably detailed research studies. As presented in this study, the water isotopic ratios of the natural water samples could be helpful in identifying the source and the routes of the river waters, and evaluating the proportion of the individual water sources.

Except for the Panas River Basin and the area associated with it, the river water was likely composed of the meteoric water and the return flow from paddy fields. Based on the water isotopic relationship, the return flow from paddy fields considerably contributed to the river flow to the extent beyond its area ratio to the total basin area, especially in the dry season.

The topography of Bali Island is basically very steep and the lengths of all of the rivers on this island are very short; therefore, the time required for water to flow on the ground surface from the topmost to the river mouth is only 1 or 2 days. In this situation, paddy rice agriculture allows rainwater and irrigation water from the river to remain in the basin for much longer times due to ponding in the paddy plots. This leads to an abundant return flow of water from the paddy fields even in the dry season. In other words, the water management in paddy fields, namely paddy irrigation, can significantly contribute to the river flow.

Acknowledgements We wish to thank Dr. I Wayan Budiasa and Mr. Ida Bagus Santika for support on hydrological survey in the field. This research work was also supported by the Research Institute for Humanity and Nature (RIHN), "Designing Local Frameworks for Integrated Water Resources Management" Project (C-09-Init).

References

Alley RB, Cuffey KM (2001) Oxygen- and hydrogen-isotopic ratios of water in precipitation: beyond paleothermometry. Rev Mineral Geochem 43(1):522–527

Craig H (1961) Isotopic variations in meteoric waters. Science 133:1702–1703

Kayane I (ed) (1992) Water cycle and water use in Bali Island. Dissertation, Institute of Geoscience, University of Tsukuba

Kendall C, McDonnell JJ (eds) (1998) Isotope tracers in catchment hydrology. Elsevier, Amsterdam

Maruyama S, Tada Y (2014) Comparison of water isotope analysis between cavity ring-down spectroscopy and isotope ratio mass spectrometry. Geochem J 48:105–109

OECD (2006) Water and agriculture sustainability, markets and policies. OECD Publishing, Paris

Saptomo SK, Chadirin Y, Setiawan BI (2015) Quantifying water balance of Subak paddy field based of continuous field monitoring. J Teknologi (Sci Eng) 76(15):53–59

Shimano Y (1994) Characteristics of hydro-geomorphology in the volcanic island of Bali, Indonesia. Dissertation, Bulletin of Bunsei University of Art 6:7–35 **(in Japanese with English abstract)**